Extraction of Urban Built-up Land Features from Landsat Imagery Using a Thematic-oriented Index Combination Technique

Hanqiu Xu

Abstract

This paper proposes a technique to extract urban built-up land features from Landsat Thematic Mapper (TM) and Enhanced Thematic Mapper Plus (ETM+) imagery taking two cities in southeastern China as examples. The study selected three indices, Normalized Difference Built-up Index (NDBI), Modified Normalized Difference Water Index (MNDWI), and Soil Adjusted Vegetation Index (SAVI) to represent three major urban land-use classes, built-up land, open water body, and vegetation, respectively. Consequently, the seven bands of an original Landsat image were reduced into three thematic-oriented bands derived from above indices. The three new bands were then combined to compose a new image. This considerably reduced data correlation and redundancy between original multispectral bands, and thus significantly avoided the spectral confusion of the above three land-use classes. As a result, the spectral signatures of the three urban land-use classes are more distinguishable in the new composite image than in the original seven-band image as the spectral clusters of the classes are well separated. Through a supervised classification, a principal components analysis, or a logic calculation on the new image, the urban built-up lands were finally extracted with overall accuracy ranging from 91.5 to 98.5 percent. Therefore, the technique is effective and reliable. In addition, the advantages of SAVI over NDVI and MNDWI over NDWI in the urban study are also discussed in this paper.

Introduction

Urban spatial areas have expanded in an accelerated speed during the last five decades, and rates of urban population growth are higher than the overall growth in most countries because urban areas are the locus of economic activity and transportation nodes (Masek *et al.*, 2000). Expanded urbanized areas encroached on surrounding valuable natural lands such as paddy fields, forestlands, or wetlands (Xu *et al.*, 2000). Urban areas are dominated by built-up lands with impervious surfaces, and therefore the conversion of the nature lands into these impervious built-up lands may have significant impacts on the ecosystem, hydrologic system, biodiversity, and local climate which can result in the negative aspects such as the urban heat island phenomenon. The study of urban spatial expansion and the resultant urban heat island phenomenon always needs accurate data on urban built-up areas such as the size, shape, and spatial context. Therefore, a technique is required to quickly reveal the data. Timely availability of the data is of great importance for urban planners and decision makers. Fortunately, satellite remote sensing technology offers considerable promise to meet this requirement. With different spatial and spectral resolutions, the satellite observations can provide globally consistent and repetitive measurements of the Earth's surface conditions. The objective of this study is to develop a new technique to extract urban built-up land features from Landsat Thematic Mapper (TM) and Enhanced Thematic Mapper Plus (ETM+) imagery. This would allow urban planner and decision makers to timely understand and evaluate urban growth with related land-cover changes and be aware of the sustainable usage of the invaluable nature lands.

Many researchers have made use of remote sensing imagery to discriminate urban lands from non-urban lands. A popular method for the definitions of urban areas started with conventional multispectral classification. However, this may not produce satisfactory accuracy, normally less than 80 percent, due to spectral confusion of the heterogeneous urban built-up land class. Therefore, many studies have not only used a single classification method to extract the urban built-up lands but also combined different methods to improve the extraction. Masek *et al.* (2000) identified urban built-up areas of the Washington D.C. metropolitan area from multi-date Landsat images based on an NDVI-differencing approach with the assistance of an unsupervised classification and achieved overall accuracy of 85 percent. Xu (2002) extracted urban built-up lands of Fuqing City in southeastern China by a combination of signature analysis and supervised classification. Based on the analysis of spectral response differences between built land and various non-built classes within multispectral bands, urban land information was extracted and then integrated with a classification layer to generate a final product with improved accuracy. Zhang *et al.* (2002) integrated a road density layer with spectral bands for the post-classification change detection of Beijing, China. This greatly reduced spectral confusion and increased accuracy of the change detection. Zha *et al.* (2003) proposed the Normalized Difference Built-up Index using TM4 and TM5 and applied it in extracting urban areas of Najing City of China

College of Environment and Resources, Fuzhou University, Key Laboratory of Data Mining and Information Sharing, China's Ministry of Education, Fuzhou, Fujian 350108, China (fdy@public.fz.fj.cn).

Photogrammetric Engineering & Remote Sensing
Vol. 73, No. 12, December 2007, pp. 1381–1391.

0099-1112/07/7312–1381/$3.00/0

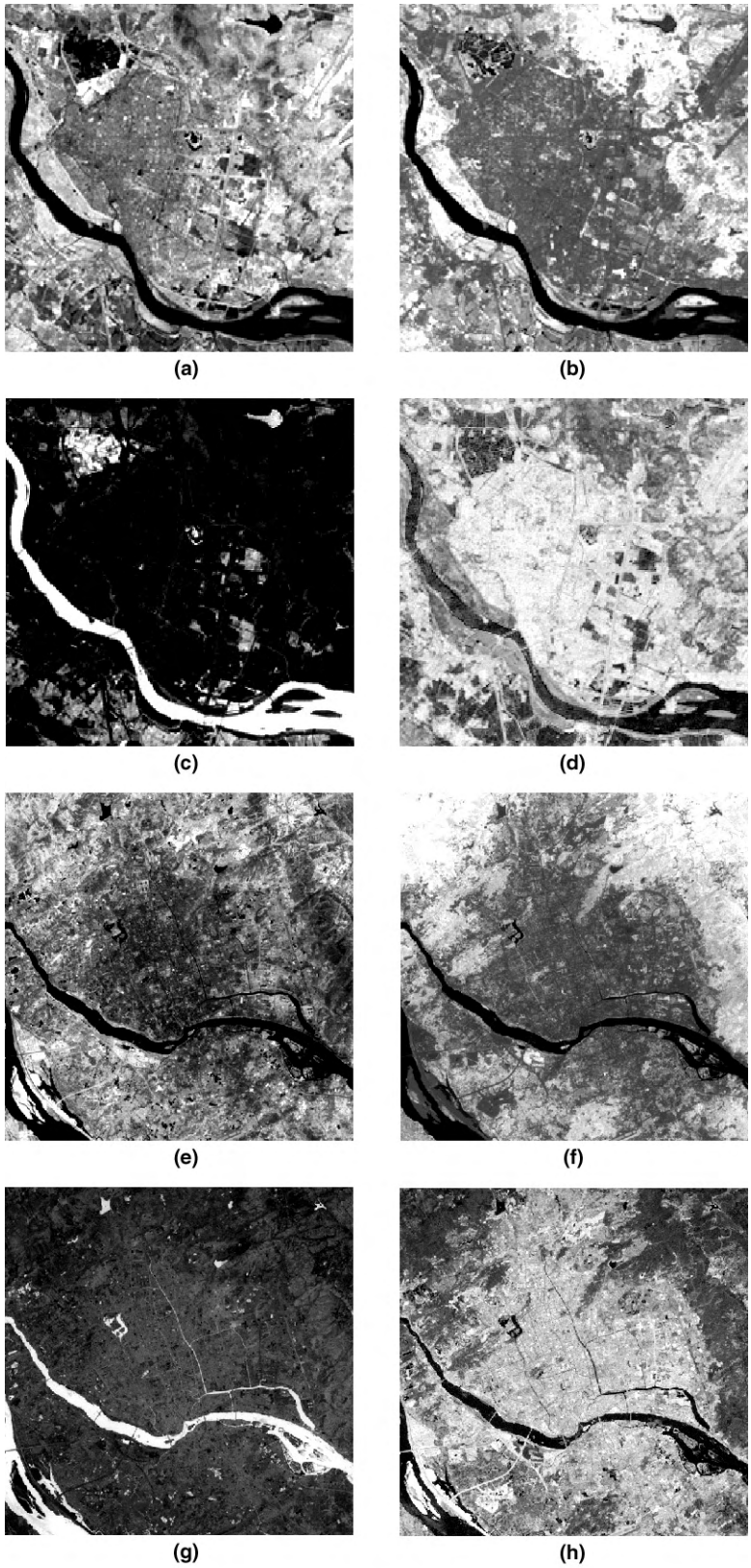

Figure 1. Landsat TM image of Quanzhou area (a) with its derived SAVI (b), MNDWI (c), and NDBI (d) images, and ETM+ image of Fuzhou area (e) with its derived SAVI (f), MNDWI (g), and NDBI (h) images (North to the top; sizes of Quanzhou and Fuzhou images is 7.71 km × 7.71 km and 16.7 km × 16.7 km, respectively). A color version of this figure is available at the ASPRS website: **www.asprs.org**.

from a Landsat TM image. The index-derived map was further filtered using the NDVI to remove the vegetation noise, as the vegetation information was mixed with the extracted built-up lands. Guindon *et al.* (2004) mapped urban land with a combination of spectral and spatial information. This started with an unsupervised classification and a segment-based classification, respectively. The two classifications were then merged using rules to generate a final product with enhanced land-use classes and accuracy. More recently, Xian and Crane (2005) measured urban land expansion of the Tampa Bay watershed of Florida by using a regression tree algorithm to map urban impervious surfaces and an unsupervised classification to reveal related land-cover classes which achieved an accuracy greater than 85 percent.

A new technique is proposed in this paper for the extraction of urban build-up land information. The extraction is mainly based on a new image derived from three thematic indices, Soil Adjusted Vegetation Index (SAVI), Modified Normalized Difference Water Index (MNDWI), and Normalized Difference Built-up Index (NDBI). The technique is demonstrated through the extraction of urban built-up lands of Quanzhou and Fuzhou Cities in southeastern China from Landsat TM/ETM+ images.

Methods

Study Area and Remote Sensing Data Source

The remotely sensed data used in this test are a Landsat TM image (path 119, row 43, covering Quanzhou City) acquired on 17 May 1996 and an ETM+ image (path 119, row 42, covering Fuzhou City) acquired on 29 May 2003. The images are cloud-free and have excellent quality. Sub-scenes covering the test cities were further extracted from the two images (Figure 1a and 1e). No preprocessing of the images was carried out except a simple atmospheric scattering correction procedure using the Dark Object Subtraction (DOS) method. However, to maintain data objectivity and avoid introducing uncertainty, the data provided in following Tables 1 through 5 are based on the original raw images. Nevertheless, the extracted results from both raw and DOS-corrected images were provided in Table 6 to examine whether there are any differences between them. Also, the means mentioned in following tables and figures are all calculated based on related classified images.

Two cities are all located in Fujian Province. Fuzhou City is the capital of the province, geographically ranging from 119°13′ to 119°25′ East and 25°59′ to 26°08′ North, and had a total urban area of approximately 119 km^2 in the study year of 2003. While Quanzhou City, about 200 km south to the Fuzhou, ranges from 118°32′ to 118°37′ East and 24°52′ to 24°58′ North and had a total urban area of approximately 24 km^2 in the study year of 1996.

Production of Index-derived Images

An urban area is a complex ecosystem composed of heterogeneous materials. Nevertheless, there are still some generalizing components among these materials. Ridd (1995) divided the urban ecosystem into three components, i.e., impervious surface material, green vegetation, and exposed soil while ignoring water surfaces. However, the open water is an important component of the urban surface and has to be taken into consideration in this study. Accordingly, the urban land-use was grouped into the other three generalized categories, i.e., built-up land, vegetation, and open water (Figure 2). Based on these three elements, three indices, NDBI, SAVI, and MNDWI, were selected in this study to represent above three major land-use classes, respectively.

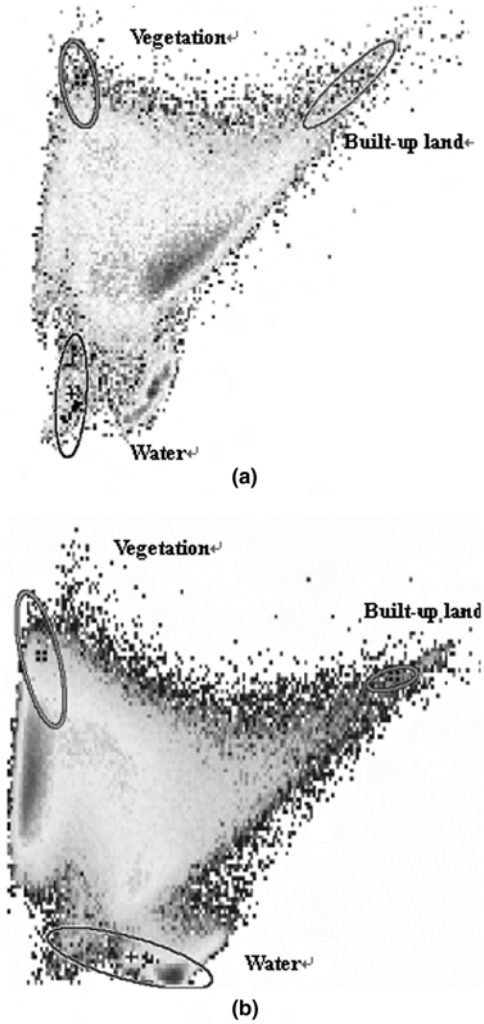

Figure 2. Scattergrams of Red (*x*-axis)-NIR (*y*-axis) spectral space with three major urban land-use classes located at the three angles of the near-triangular space: (a) Quanzhou image, and (b) Fuzhou image.

SAVI-derived Vegetation Image

There are various vegetation indices to enhance vegetation information in remote sensing imagery usually by ratioing a near-infrared (NIR) band to a red band. This takes advantage of the high vegetation reflectance in NIR spectral range such as TM band 4 and high pigment absorption of red light, such as TM band 3 (Jensen, 2000). Although nearly everyone working with the remote sensing of vegetation knows the Normalized Difference Index (NDVI), this study employed SAVI to highlight vegetation features due to its advantage over NDVI when applied in an area with low plant cover such as the urban areas. SAVI can work in the area with plant cover as low as 15 percent, while NDVI can only work effectively in the area with plant cover above 30 percent (Ray, 1994).

The SAVI is calculated using the following equation (Huete, 1988):

$$SAVI = \frac{(NIR - Red)(1 + l)}{NIR + Red + l} \quad (1)$$

where l is a correction factor ranging from 0 for very high densities to 1 for very low densities. A value of 0.5 was used in this study to produce enhanced vegetation image as the study region has an intermediate vegetation density (Figure 1b and 1f).

It is noted in this test that SAVI is really more sensitive than NDVI in detecting vegetation in the low plant-covered areas due largely to the increased data dynamic ranges of the images (Table 1). The increased dynamic range is 85 when the difference is rescaled between 0 and 255 to provide output as unsigned 8-bit data. The increase in the range can make the discrimination of vegetation from built-up land or water easier. For example, the NDVI difference between vegetation and built-up land in Quanzhou image is 0.61, whereas the SAVI difference between them is 0.92 (Table 2). A 0.31 or 50 percent contrast increase would greatly help in the separation of these two classes.

MNDWI-derived Water Image

McFeeters (1996) proposed the Normalized Difference Water Index (NDWI) to delineate open water features, which is expressed as follows:

$$NDWI = \frac{GREEN - NIR}{GREEN + NIR} \quad (2)$$

where *GREEN* is a green band such as TM2, and *NIR* is a near infrared band such as TM4.

This index maximizes reflectance of water by using green light wavelengths and minimizes low reflectance of NIR by water features while taking advantage of the high reflectance of NIR by vegetation and soil features. As a result, water features are enhanced owing to having positive values and vegetation and soil are suppressed due to having zero or negative values.

However, the applications of the NDWI in the water regions with built-up land background like the cases of Quanzhou and Fuzhou cities were not as successful as expectation. The extracted water information in these regions was often mixed up with built-up land noise because many built-up lands also have positive values in the NDWI-derived image. The signature features of built-up land in green band (TM2) and NIR band (TM4) shown in Figure 3 are similar with those of water, i.e., they both reflect green light more than reflect near infrared light. Consequently, the computation of the NDWI also produces a positive value for built-up land just as for water. Table 3 shows that the built-up land class in both Quanzhou and Fuzhou images has positive mean values. To remedy this problem, Xu (2005) modified the NDWI by using a middle infrared (MIR) band such as TM5 to substitute the NIR band in the NDWI. The modified NDWI (MNDWI) is expressed as follows:

$$MNDWI = \frac{GREEN - MIR}{GREEN + MIR}. \quad (3)$$

Figure 3 shows that the mean of TM5 is much greater than that of TM2. Therefore, if a MIR band is used instead of a NIR band, the built-up land should have negative values while keeping the water values positive. Accordingly, the enhanced water features will no longer have built-up land noise in a MNDWI image. This substitution has no impact on vegetation, as vegetation still has negative value when calculated using Equation 3 (Figure 3). Therefore, this test employed MNDWI instead of NDWI to enhance water features in the built-up land-dominated urban area (Figure 1c and 1g).

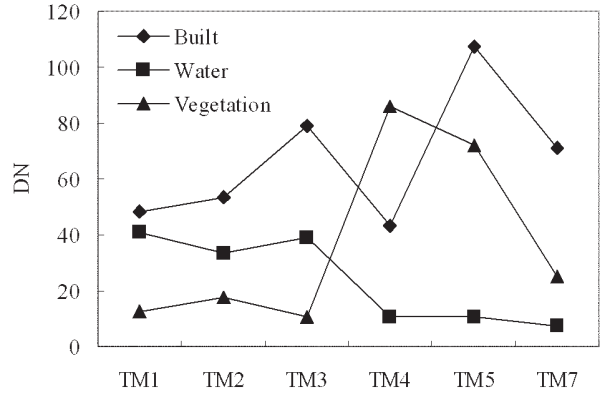

Figure 3. Spectral signatures represented by the mean of three urban land-use classes taking the Quanzhou image as an example.

TABLE 1. DYNAMIC RANGES OF NDVI AND SAVI OF THE TEST IMAGES

	Quanzhou image			Fuzhou image		
	Minimum	Maximum	Dynamic range	Minimum	Maximum	Dynamic range
SAVI	−0.902	0.979	1.881	−0.911	0.633	1.544
NDVI	−0.606	0.654	1.260	−0.609	0.423	1.032
Dynamic range difference			0.621			0.512
Difference rescaled			85			85

TABLE 2. THE MEAN OF NDVI AND SAVI OF THE THREE LAND-USE CLASSES WITH THEIR DIFFERENCES IN THE STUDY AREAS

		Mean			Difference		
		NDVI	SAVI		NDVI	SAVI	Increase
Quanzhou	Vegetation	0.51	0.77	Vegetation versus Built-up	0.61	0.92	0.31
	Built-up	−0.10	−0.15	Built-up versus Water	0.32	0.51	0.19
	Water	−0.42	−0.66	Water versus Vegetation	0.93	1.43	0.50
Fuzhou	Vegetation	0.29	0.42	Vegetation versus Built-up	0.59	0.87	0.28
	Built-up	−0.30	−0.45	Built-up versus Water	0.21	0.31	0.10
	Water	−0.51	−0.76	Water versus Vegetation	0.80	1.18	0.38

TABLE 3. THE MEAN OF NDWI AND MNDWI AND DIFFERENCE BETWEEN BUILT-UP LAND AND WATER

		Mean			Difference		
		NDWI	MNDWI		NDWI	MNDWI	Increase
Quanzhou	Built-up land	0.07	−0.35	Built-up land versus Water	0.35	0.95	0.60
	Water	0.42	0.60				
Fuzhou	Built-up land	0.19	−0.02	Built-up land versus Water	0.34	0.67	0.33
	Water	0.53	0.65				

Moreover, MNDWI can enhance the contrast between built-up land and water much more than NDWI because built-up lands reflect MIR radiation much higher than NIR radiation (Figure 3). The increase in difference between them would help the delineation of these two classes (Table 3).

NDBI-derived Built-up Land Image

The built-up land image (Figure 1d and 1h) was produced using the NDBI of Zha *et al.* (2003) with the following equation:

$$NDBI = \frac{MIR - NIR}{MIR + NIR}. \quad (4)$$

The development of the index was based on the unique spectral response of built-up lands that have higher reflectance in MIR wavelength range than in NIR wavelength range. However, this is not always the case. Some studies showed that the reflectance for certain types of vegetation over the band pass of TM5 increased as leaf water content decreased (Cibula *et al.*, 1992; Gao, 1996). The drier vegetation can even have higher reflectance in MIR wavelength range than in NIR range (Gao, 1996), resulting in positive values in NDBI imagery for these plants. This study also found that the many vegetated areas have positive NDBI values, especially in Fuzhou's NDBI image where the mean of vegetation is 0.01. Furthermore, in some circumstances, water with high suspended matter concentration (SMC) can also reflect MIR stronger than NIR because the reflectance peak shift to longer wavelength regions as the suspended matter increase. Therefore, the drier vegetation and water with high SMC will have positive NDBI values when computed using Equation 4 and present as noise in a NDBI image. Consequently, the contrast of the NDBI image is not so good as SAVI and MNDWI images (Figure 1), because many pixels of vegetation and water areas having positive NDBI values show medium gray tones and present as noise mixed with built-up features. Wu *et al.* (2005) employed NDBI to extract urban built-up lands of Xi'an City of China and obtained a low accuracy of 78.7 percent. A similar situation was also encountered in this study (see discussion later). These suggest that the urban built-up land features could not be extracted merely based on a NDBI image. This is why this study combines the NDBI with SAVI and MNDWI to extract urban built-up land features. This combination can remove the vegetation and water noise, and hence improve the extraction accuracy.

Extraction of Urban Built-up Land Features

After producing SAVI, MNDWI, and NDBI images, a new image dataset was created, which used these three new images as three bands. The further extraction of urban built-up land was carried out based on this new dataset. The change from an original seven-multispectral-band image into the three-thematic-band image largely reduces correlation among three bands (Table 4). Consequently, three major urban land-use classes, vegetation, water, and built-up land are well separated (Figure 4). Compared with the original image, moreover, spectral signature analysis was also greatly simplified owing to the reducing of band-dimensions (Figure 3 and Figure 5).

TABLE 4. CORRELATION VALUES OF THE TWO NEW IMAGES COMPOSED OF SAVI-, NDBI-, AND MNDWI-DERIVED BANDS

	Quanzhou image			Fuzhou image		
	SAVI	NDBI	MNDWI	SAVI	NDBI	MNDWI
SAVI	1.000	−0.107	−0.558	1.000	−0.378	−0.638
NDBI	−0.107	1.000	−0.756	−0.378	1.000	−0.461
MNDWI	−0.558	−0.756	1.000	−0.638	−0.461	1.000

Three methods were used to extract built-up land features from the new images composed of the three thematic-oriented bands, which are principal components analysis (PCA), logic calculation, and supervised classification methods.

PCA is a method that examines principal components eigenvector loadings to decide which of the PC images will concentrate information related directly to the theoretical spectral signatures of specific target materials. The technique is able to predict whether the target material is represented by bright or dark pixels in the relevant PC image according to the magnitude and sign of the eigenvectors. Table 5 describes the PC transformation on the new images based on the covariance matrix and is the base for identifying which PC has the greatest loadings (values) for NDBI band (representing the built-up land class), but that also has opposite signs (+ or −) with SAVI and MNDWI bands. It is obvious that the built-up lands cannot be identified from PC3 as all three input bands have positive loadings in the two images, and is also difficult to be separated from vegetation in PC1 of the two images because both NDBI and SAVI bands in Quanzhou image have close positive loadings, and the NDBI band of Fuzhou image only has a small loading (0.014). Therefore, the built-up lands can only be mapped by PC2 based on a strong positive or negative loading with an opposite sign from SAVI and MNDWI bands. The negative sign of the loading for NDBI-band in Quanzhou image indicates that the built-up lands will be present by dark pixels. Accordingly, by negating (i.e., multiplying by −1) PC2 image, built-up lands of the image were mapped as bright pixels. Finally, a threshold value (Table 6) was used to extract built-up features from the PC2 image to form a binary-image with the built-up land class assigned a value of 1 and all non-built-up land classes a value of 0 (Figure 6a and 6f).

The second method is an "if-then-else" logic calculation through a band spectral signature analysis. A simple rule-based logic tree is used to segment urban built-up lands from non-urban built-up lands. Figure 5 illustrates the signatures of the three new bands in the two index-derived images. A distinct feature is that the mean values of band 2 (NDBI-band) of both new images are all greater than those of

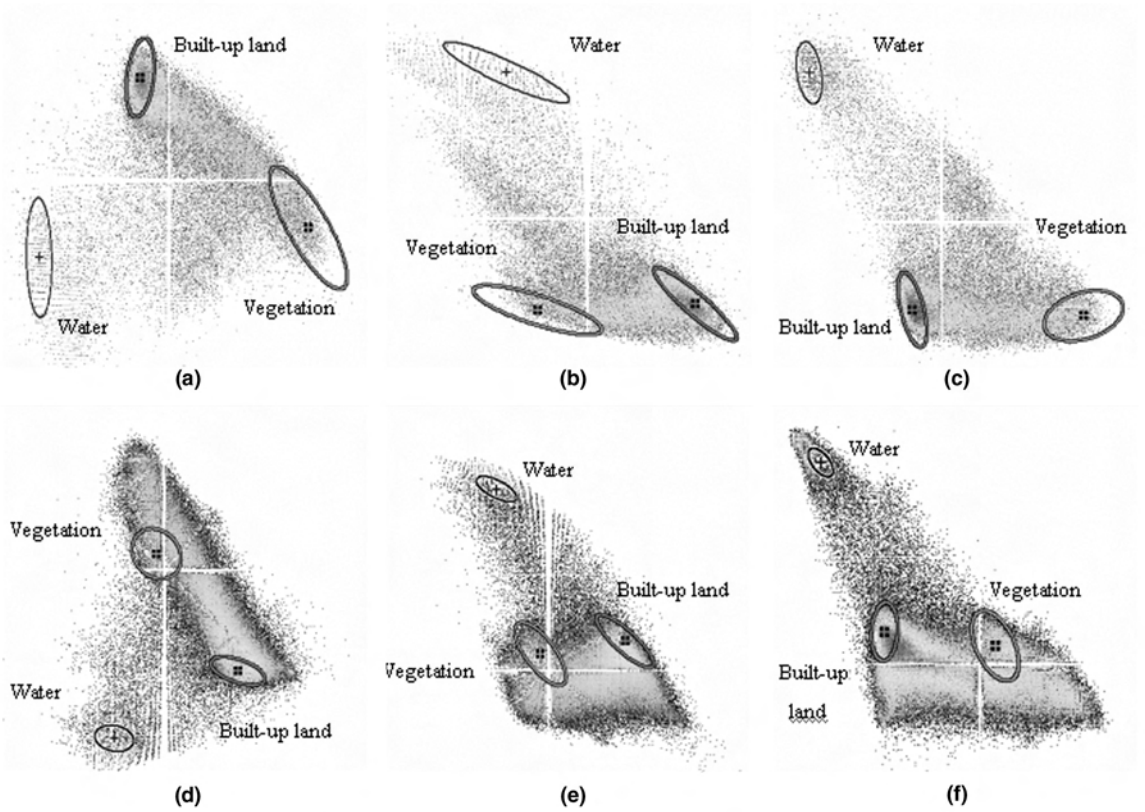

Figure 4. Scattergrams of spectral feature space of the two new three-band images derived from their original seven-band images showing well-separated water, urban and vegetation classes: (a) SAVI (*x*-axis)-NDBI (*y*-axis), (b) NDBI (*x*-axis)-MNDWI (*y*-axis), (c) SAVI (*x*-axis)-MNDWI (*y*-axis) spaces of the Quanzhou image, (d) NDBI (*x*-axis)-SAVI (*y*-axis), (e) NDBI (*x*-axis)-MNDWVI (*y*-axis), and (f) SAVI (*x*-axis)-MNDWI (*y*-axis) spaces of the Fuzhou image.

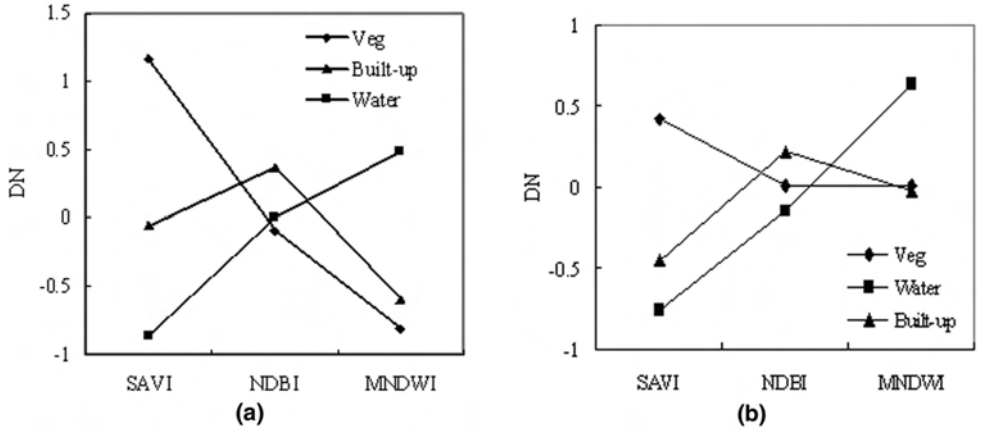

Figure 5. Simplified spectral signatures represented by the mean of three major land-use classes of (a) Quanzhou, and (b) Fuzhou new images.

TABLE 5. PRINCIPAL COMPONENTS ANALYSIS ON THE TWO NEW THREE-BAND IMAGES

		Quanzhou image			Fuzhou image		
		PC1	PC2	PC3	PC1	PC2	PC3
Eigenvectors	SAVI-band	0.571	0.72	0.394	−0.894	−0.311	0.322
	NDBI-band	0.461	−0.679	0.571	0.014	0.700	0.714
	MNDWI-band	−0.679	0.144	0.72	0.447	−0.011	0.621

TABLE 6. SUMMARY OF ACCURACY VALIDATION RESULTS

			Quanzhou image					Fuzhou image				
No.	Extraction method		built	non-built	total	Overall accuracy	Kappa	built	non-built	total	Overall accuracy	Kappa
1	**Logic calculation**	built	131	12	143	93.0%	0.836	120	0	120	98.5%	0.969
	raw image	non-built	2	55	57			3	77	80		
		total	133	67	200			123	77	200		
2	**Logic calculation**	built	131	10	141	93.9%	0.861	120	8	128	94.5%	0.882
	DOS-corrected image	non-built	2	57	59			3	69	72		
		total	133	67	200			123	77	200		
3	**PC2**	built	131	4	135	97.0%	0.932	122	16	138	91.5%	0.813
	raw image,	non-built	2	63	65			1	61	62		
	thresholded at 0.231 for Quanzhou, 0.139 for Fuzhou	total	133	67	200			123	77	200		
4	**PC2**	built	129	9	138	93.5%	0.851	118	3	121	96.0%	0.9159
	DOS-corrected image,	non-built	4	58	62			5	74	79		
	thresholded at 0.409 for Quanzhou, 0.3 for Fuzhou	total	133	67	200			123	77	200		
5	**Supervised classification**	built	132	15	147	92.0%	0.811	119	2	121	97.0%	0.937
	raw image	non-built	1	52	53			4	75	79		
		total	133	67	200			123	77	200		
6	**Supervised classification**	built	133	15	148	92.5%	0.822	119	0	119	98.0%	0.958
	DOS-corrected image	non-built	0	52	52			4	77	81		
		total	133	67	200			123	77	200		
7	**Supervised classification***	built	123	27	150	81.5%	0.557	123	47	170	76.5%	0.439
	original image	non-built	10	40	50			0	30	30		
		total	133	67	200			123	77	200		
8	**NDBI**	built	131	30	161	84.0%	0.599	123	40	163	80.0%	0.532
	raw image,	non-built	2	37	39			0	37	37		
	thresholded at 0.0	total	133	67	200			123	77	200		
9	**NDBI**	built	131	33	164	82.5%	0.556	123	75	198	62.5%	0.032
	DOS corrected image,	non-built	2	34	36			0	2	2		
	thresholded at 0.0	total	133	67	200			123	77	200		

*The accuracies obtained from the raw and DOS-corrected images are identical.

band 1 (SAVI-band) and band 3 (MNDWI-band). Therefore, a simple logic statement can easily extracted urban built-up lands from the image owing to its much simpler signatures than those of original image (Figure 3). The logic calculation can be expressed in ER Mapper™as follows:

If Band 2 > Band 1 and Band 2 > Band 3 then 1 Else 0.

The pixels of built-up lands had a value of 1 after the logic calculation and resultant image was also a binary-image. The urban built-up lands of Quanzhou were so extracted (Figure 6b). However, Figure 5b shows that the difference between means of built-up land class and vegetation class in NDBI-band of Fuzhou image is not as large as that of Quanzhou image (Figure 5a). This might cause confusion between built-up land and vegetation classes in Fuzhou image if only above logic statement is used for the extraction, and the result would not be as good as that of Quanzhou image. Therefore, one more condition was added in the statement as follows to assist the extraction:

If Band 1 < −0.344 and Band 2 > Band 3 then 1 Else 0.

The maximum of built-up land class in band1 (SAVI-band) of Fuzhou image is −0.343, whereas the minimum of vegetation class in that band is −0.182. Therefore, using −0.344 as a threshold value can help avoid the confusion between vegetation and built-up land classes and greatly increase the extraction accuracy (see sections below).

The supervised classification was performed using a maximum likelihood algorithm based on the signatures of training regions (Figure 4). The built-up lands were extracted directly from the classified image to form a binary-image with the built-up land class assigned a value

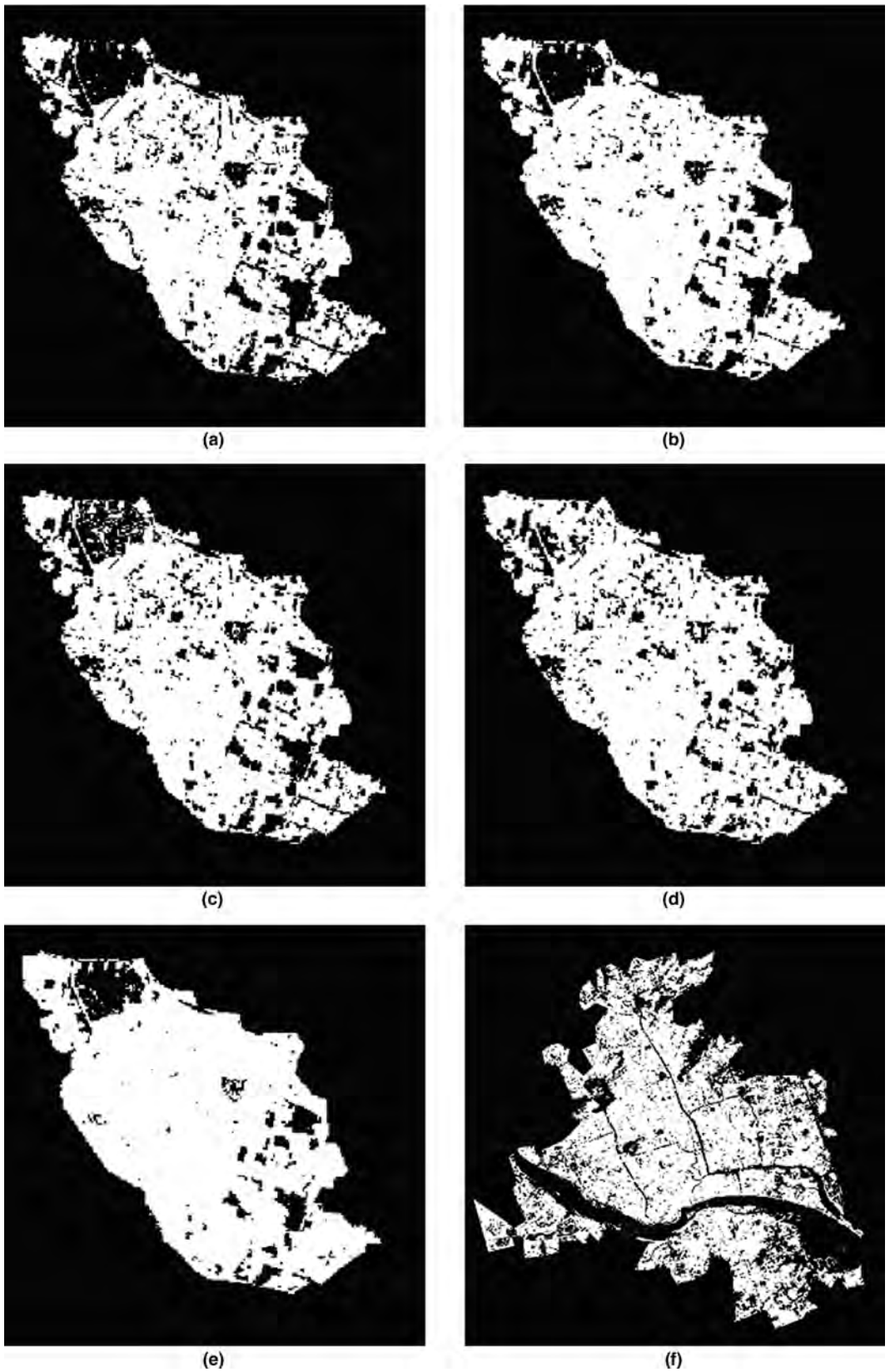

Figure 6. Urban built-up land extraction results from Quanzhou (a through e) and Fuzhou (f through j) using (a) PC2 method, (b) logic calculation method on DOS-corrected image, (c) supervised classification method, (d) supervised classification on the original image, (e) NDBI method, (f) PC2 method on DOS-corrected image,

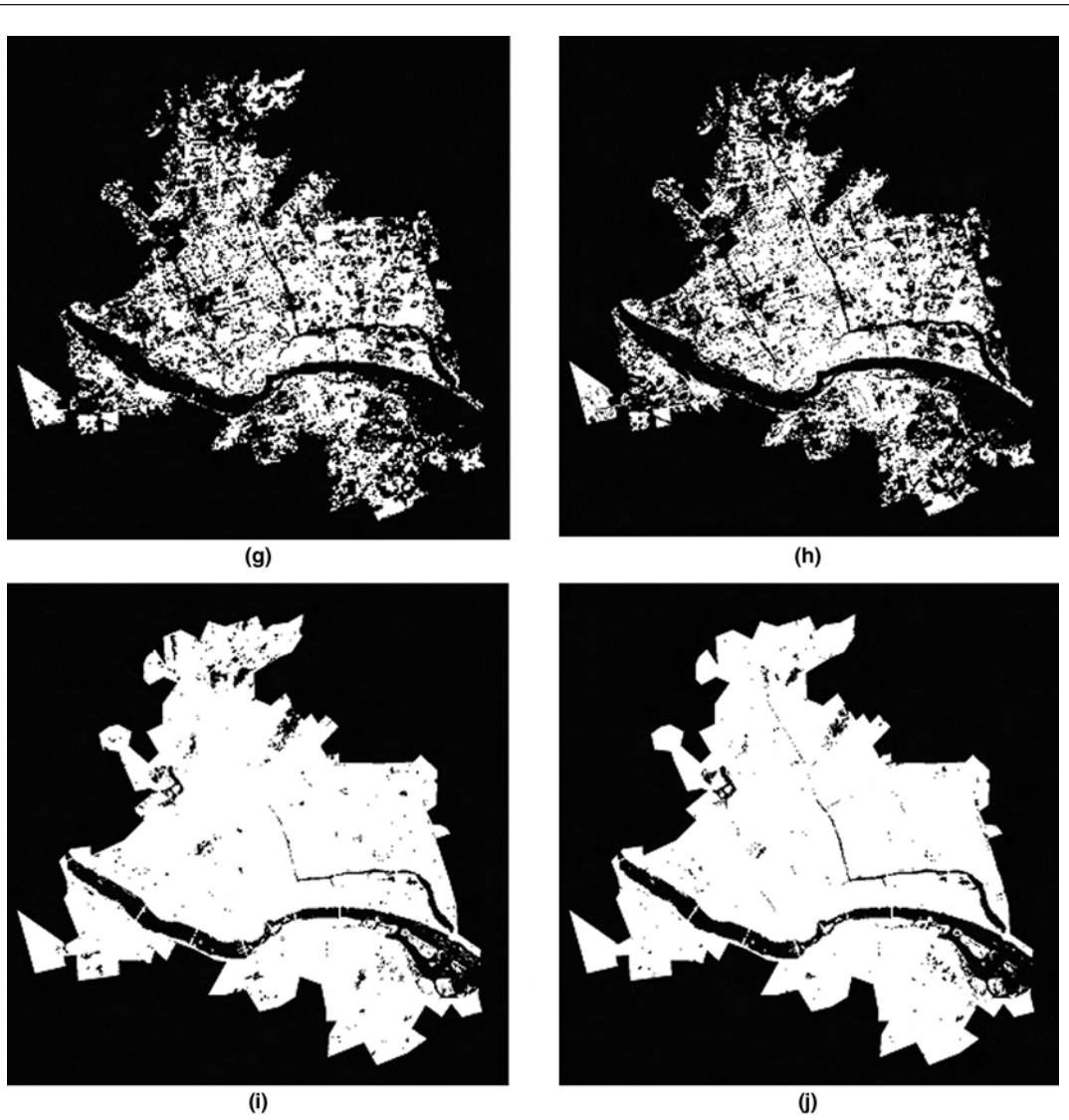

Figure 6. (Continued) (g) logic calculation method, (h) supervised classification on DOS-corrected image, (i) supervised classification on the original image, and (j) NDBI method. Only higher accuracy image of each method is shown.

of 1 and all non-built-up land classes to a value of 0 (Figure 6c and 6h).

Finally, non-urban areas of the two cities were masked out using a vector polygon representing each city's outline, and only the built-up lands within the urban region were left as urban built-up lands (Figure 6).

Accuracy Assessment

To compare the extraction accuracy, the original seven-band Landsat TM image was classified using a supervised maximum likelihood classification method with the same training regions as those used in previous classification (Figure 4). In addition, extraction based only on a NDBI image was also carried out for the comparison. The urban built-up lands were extracted from the NDBI image when the digital numbers of pixels were greater than a default threshold value of 0. The extracted results from the supervised classification and the NDBI image were also made into binary images (Figure 6d, 6e, 6i, and 6j).

Two SPOT images with finer spatial resolution were used as reference datasets from which the extraction results were compared. One used for Fuzhou area is a 10 m SPOT-5 multispectral image and acquired on 13 December 2003. The other for Quanzhou area is a PAN image with 10 m resolution and was acquired on 18 May 1996, one day after the Landsat TM image collected. The Quanzhou's SPOT PAN and TM images were fused together using the Brovey algorithm to produce a 10 m multispectral image. The extracted binary-images were overlaid on the RGB-colored SPOT image, and then visually inspected pixel by pixel. A random sampling method was used, and a total of 200 pixels were sampled. All resultant binary-images were assessed using the same samples. The extraction results from both raw images and DOS-corrected images were all evaluated to see whether there is any difference between them. Table 6 summarizes the accuracy assessment results and clearly shows that the overall extraction accuracy of urban built-up land features based on the three-thematic-band image are higher than those based on the original image or on the NDBI image. The accuracy from the

new images ranges from 91.5 to 98.5 percent with Kappa coefficients from 0.813 to 0.969, while overall accuracy of the NDBI-extracted results or original image are all less than 85 percent with Kappa coefficients less than 0.6. This indicates that the thematic-oriented band compression technique can achieve much better extraction results.

Discussion

Table 6 shows that all three methods described earlier can extract urban built-up lands from the new three-thematic-band images with high overall accuracy (on an average close to 95 percent in the 12 tests). The best overall accuracy, 98.5 percent, was achieved through the logic calculation method, which is the fastest, easiest, and most objective one among the three methods. One simple logic statement can generally achieve a quite good extraction result like in Quanzhou case. Nevertheless, one more condition added can considerably increase extraction accuracy such as in the Fuzhou case, as it well discriminate vegetation from built-up land. Consequently, no confusion was found between them in the sampling procedure of accuracy assessment (Table 6). The threshold value used in the conditional statement was just simply taken from the maximum of the built-up land class in SAVI-band and did not need to bother to find it. The method also has the highest average overall accuracy (94.98 percent) among the three considered.

The PC2 can also get high accuracy up to 97 percent. This is probably owing to the fact that the contrast between built-up land and vegetation or water in the PC2 image is further enlarged as indicated by their contributions to PC2 and by opposite signs of the loadings (Table 5). Therefore, the method can effectively enhance built-up land features while depressing water and vegetation information in the PC2 image.

The conventional supervised classification on the new three-band image can produce very high accuracy up to 98 percent, while the same classification method performed on the original image can only have maximum accuracy of 81.5 percent. The good separation of the spectral clusters of the three urban categories in the new three-band image (Figure 4) greatly reduced the confusion between them, and thus considerably improves the classification accuracy. The supervised classification on the raw and DOS-corrected original seven-band images got the identical results because the DOS method is only shift the origin of the dataset as indicated by Song *et al.* (2001).

The accuracy based only on the NDBI image using a default threshold value of 0 is lower than 85 percent, the minimum acceptable overall accuracy proposed by Anderson *et al.* (1976). Step-by-step adjusting the threshold value can reach higher overall accuracy but never exceeds 88.5 percent. The confusion matrix in Table 6 shows that the error is obviously caused by high overestimation of the non-built-up lands. Visual inspection of extraction result (Figure 6e and 6i) can find that the confusion mainly lies between built-up land and vegetation classes. As discussed earlier, besides built-up lands many vegetation areas also have positive values in NDBI imagery, and thus made the confusion with the built-up land areas. This directly resulted in the low accuracy of the extraction.

It seems no significant different between the extraction results from raw and DOS-corrected imagery and no rule can be found within them. In Quanzhou's case, the average accuracy of raw image is slightly greater than that of DOS-corrected image (94.0 percent versus 93.3 percent). While the situation is changed in Fuzhou case, and the average accuracy of DOS-corrected image is 0.5 percent higher than that of raw image (96.17 percent versus 95.67 percent).

Conclusions

The original seven bands of a Landsat TM/ETM+ image can be reduced into three thematic-oriented bands to produce a new image. The reducing was not carried out through the conventional Principal Components Analysis method. Instead, the three new bands were generated directly from three thematic indexes, SAVI, MNDWI, and NDBI. This dramatically reduced data correlations and redundancy between multispectral bands, significantly avoided the spectral confusion between the land-use classes, and thus largely improved the extraction accuracy. Besides, using SAVI and MNDWI instead of NDVI and NDWI also contribute to the improvement because this can significantly increase the spectral contrast between different land-use classes. Consequently, the high accuracy of extraction of urban built-up land features was achieved through a simplified band spectral signature analysis, a PCA, or a maximum likelihood supervised classification. Among the three methods, the logic calculation method can generally achieve higher accuracy. Moreover, the method is fast and objective, as it does not need to manually test a threshold value repeatedly. The PCA and supervised classification methods can also have high extraction accuracy, but are more subjective and time-consuming due to the attempt on selecting a suitable threshold value or defining training regions.

There appears to be no need to do DOS-correction for the image to be used for extraction, as it still cannot be proved that the DOS-corrected imagery can get much better extraction results.

Acknowledgment

This work is supported by the National Natural Science Foundation of China (No. 40371107).

References

Anderson, J.R., E.E. Hardy, J.T. Roach, and R.E. Witmer, 1976. *A Land Use and Land Cover Classification System for Use with Remote Sensor Data*, USGS Professional Paper 964, Reston, Virginia.

Cibula, W.G., E.F. Zetka, and D.L. Rickman, 1992. Response of thematic bands to plant water stress, *International Journal of Remote Sensing*, 13(10):1869–1880.

Gao, B.C., 1996. NDWI–A normalized difference water index for remote sensing of vegetation liquid water from space, *Remote Sensing of Environment*, 58(3):257–266.

Guindon, B., Y. Zhang, and C. Dillabaugh, 2004. Landsat urban mapping based on a combined spectral–Spatial methodology, *Remote Sensing of Environment*, 92(2):218–232.

Huete, A.R., 1988. A soil-adjusted vegetation index (SAVI), *Remote Sensing of Environment*, 25(3):295–309.

Jensen, J.R., 2000. *Remote Sensing of the Environment: An Earth Resource Perspective*, Prentice Hall, Upper Saddle River, New Jersey, 544 p.

McFeeters, S.K., 1996. The use of normalized difference water index (NDWI) in the delineation of open water features, *International Journal of Remote Sensing*, 17(7):1425–1432.

Masek, J.G., F.E. Lindsay, and S.N. Goward, 2000. Dynamics of urban growth in the Washington DC metropolitan area, 1973–1996, from Landsat observations, *International Journal of Remote Sensing*, 21(18):3473–3486.

Ray, T.W., 1994. Vegetation in remote sensing FAQs, *Applications*, ER Mapper, Ltd., Perth, unpaginated CD-ROM.

Ridd, M.K., 1995. Exploring a VIS (vegetation-impervious surface-soil) model for urban ecosystem analysis through remote sensing: Comparative anatomy for cities, *International Journal of Remote Sensing*, 16(12):2165–2185.

Song, C., C.E. Woodcock, K.C. Seto, M. Pax-Lenney, and S.A. Macomber, 2001. Classification and change detection using Landsat TM data–When and how to correct atmospheric effects?, *Remote Sensing of Environment*, 75(2):230–244.

Wu, H., J. Jiang, J. Zhou, H. Zhang, L. Zhang, and L. Ai, 2005. Dynamics of urban expansion in Xi'an City using Landsat TM/ETM+ data, *Acta Geographica Sinica*, 60(1):143–150.

Xian, G., and M. Crane, 2005. Assessment of urban growth in the Tampa Bay watershed using remote sensing data, *Remote Sensing of Environment*, 97(2):203–205.

Xu, H., X. Wang, and G. Xiao, 2000. A remote sensing and GIS integrated study on urbanization with its impact on arable lands: Fuqing City, Fujian Province, China, *Land Degradation & Development*, 11(4):301–314.

Xu, H., 2002. Spatial expansion of urban/town in Fuqing and its driving force analysis, *Remote Sensing Technology and Application*, 17(2):86–92.

Xu, H., 2005. A study on information extraction of water body with the Modified Normalized Difference Water Index (MNDWI), *Journal of Remote Sensing*, 9(5):511–517.

Zha, Y., J. Gao, and S. Ni, 2003. Use of normalized difference built-up index in automatically mapping urban areas from TM imagery, *International Journal of Remote Sensing*, 24(3):583–594.

Zhang, Q., J. Wang, X. Peng, P. Gong, and P. Shi, 2002. Urban built-up land change detection with road density and spectral information from multi-temporal Landsat TM data, *International Journal of Remote Sensing*, 23(15):3057–3078.

(Received 06 February 2006; accepted 27 March 2006; revised 16 May 2006)